Available online at www.sciencedirect.com

SCIENCE DIRECT®

Remote Sensing of Environment 97 (2005) 52 – 67

Remote Sensing of Environment

www.elsevier.com/locate/rse

Estimation of the net radiation using MODIS (Moderate Resolution Imaging Spectroradiometer) data for clear sky days

Gautam Bisht [a], Virginia Venturini [a], Shafiqul Islam [a,*], Le Jiang [b]

[a] *Department of Civil and Environmental Engineering, University of Cincinnati, P.O. Box 210071, Cincinnati, OH 45221-0071, United States*
[b] *IMSG at NOAA/NESDIS, NOAA Science Center, Camp Springs, MD 20746, United States*

Received 18 October 2004; received in revised form 9 February 2005; accepted 5 March 2005

Abstract

A simple scheme is proposed to estimate instantaneous net radiation over large heterogeneous areas for clear sky days using only remote sensing observations. Our method attempts to develop an algorithm which primarily uses remote sensing information and eliminates the need for ground information as model input, by using various land and atmospheric data products available from Terra–MODIS. It explicitly recognizes the need for spatially varied parameters and provides a distributed net radiation map over large heterogeneous domain with fine spatial resolution. Since instantaneous net radiation estimates have limited scope compared to daily average values or diurnal cycle, a sinusoidal model is proposed to estimate diurnal cycle of net radiation. The sinusoidal model is capable of retrieving the diurnal variations of net radiation with a single instantaneous net radiation estimate from the satellite. Preliminary results, using data over Southern Great Plains, show good agreement with ground-based observations. It appears that the methodology presented here can estimate instantaneous and daily net radiation with comparable accuracy to those of current methods that use ground-based observations and mainly provide point estimates.

Keywords: MODIS; Net radiation; Clear sky days

1. Introduction

Net radiation (R_n) is defined as the difference between the incoming and outgoing radiation fluxes including both long- and shortwave radiation at the surface of Earth. It is a key quantity for the estimation of surface energy budget and is used for various applications including climate monitoring, weather prediction and agricultural meteorology. Remote sensing provides an unparalleled spatial and temporal coverage of land surface attributes, thus several studies have attempted to estimate net radiation (or its components) by combining remote sensing observations with surface and atmospheric data (Diak & Gautier, 1983; Gautier et al., 1980; Jacobs et al., 2000; Ma et al., 2002). R_n (coupled with soil heat flux, as 'available energy') serves as a key driving force for the evapotranspiration (ET). Over the years, various ET models have been developed that use remote sensing and ancillary surface and ground-based observations (e.g., Bastiaanssen et al., 1996; Jackson et al., 1977; Seguin et al., 1989). Several of the recent ET models primarily use remote sensing data for ET estimation (e.g., Jiang & Islam, 2001; Nishida et al., 2003; Norman et al., 2003). Yet, all these ET models require estimates of R_n.

While estimating R_n, the land surface temperature is commonly obtained directly from remote sensing observation, generally by using the split-window technique (Becker & Li, 1990). To get other components of R_n including land surface albedo, land surface emissivity, air temperature, air emissivity and incoming shortwave radiation, current approaches usually require radiative transfer models, ancillary ground measurements or assumptions about certain parameters. Ma et al. (2002) have used radiative transfer model, MODTRAN, to compute downwelling shortwave

* Corresponding author.
E-mail address: Shafiqul.Islam@tufts.edu (S. Islam).

0034-4257/$ - see front matter © 2005 Elsevier Inc. All rights reserved.
doi:10.1016/j.rse.2005.03.014

and downwelling longwave radiation, but they require radiosonde data. Similarly Hurtado and Sobrino (2001) need meteorological information about shortwave radiation, air temperature and vapor pressure. Several parameterization schemes have been developed to estimate shortwave and longwave fluxes; reviews of such parameterization schemes may be found in Niemelä et al. (2001a,b), Ellingson (1995) and Pinker et al. (1995). Numerous studies have exploited these parameterization schemes, but assumed certain parameters constant over the domain. Jacobs et al. (2000) and Nishida et al. (2003) have assumed land surface albedo and land surface emissivity to be constant, while Jiang and Islam (2001) assumed downward longwave radiation to be constant for the whole domain and computed it as an average from ground stations observations. Spatial maps of R_n can also be obtained by interpolating few ground observations of R_n. Islam et al. (2003) computed R_n for the domain by using inverse distance square weighting method from few ground station observations for the South Florida region. A major drawback of such an approach is that the R_n map thus obtained is too smooth and could not capture the spatial heterogeneity.

In this paper, we will explore an alternative methodology to capture the spatial distribution of R_n estimates over heterogeneous areas for clear sky days. The proposed approach strives to be 'stand-alone' by eliminating the need for ground data as model input and also explicitly recognizes the need for spatially varied input parameters. Earlier studies have used remote sensing observations from Geostationary Operational Environmental Satellite (GOES) and Advanced High Resolution radiometer (AVHRR). The present study uses data from Moderate Resolution Imaging Spectroradiometer (MODIS), onboard Earth Observing System (EOS) Terra satellite, launched in December 1999. MODIS has a global coverage every 1 or 2 days and 36 spectral bands (much more as compared to AVHRR which had only 5 spectral bands), thereby rendering a new opportunity for global monitoring of terrestrial ecosystems. Instantaneous net radiation (INR) estimates are obtained using various Terra–MODIS land products (land surface temperature, land surface emissivities and land surface albedo) and Terra–MODIS atmospheric data products (air temperature, dew temperature and aerosol depth). Zillman's (1972) and Prata's (1996) parameterization schemes are used to estimate downward shortwave flux and air emissivity respectively.

Many agricultural applications and models estimating ET need daily average net radiation (DANR) or diurnal cycle of net radiation. Jacobs et al. (2000) retrieved diurnal cycle of R_n using 30-min GOES observations. In this paper a sinusoidal model, similar to Lagourade and Brunet's (1983) model for surface temperature, is proposed to retrieve diurnal cycle of R_n, from which DANR is estimated later. The proposed sinusoidal model has the advantage of requiring only one satellite observation (Terra–MODIS) to reconstruct the diurnal variation for clear sky days.

The strength of the proposed methodology should be evaluated not only by how closely it reproduces surface-based point observations but also by its ability to provide a spatially consistent and distributed net radiation map over a large heterogeneous domain. To summarize, the key objectives for this paper are to develop a 'stand-alone' method, using spatially varied input parameters, to estimate R_n from remote sensing information and validate the proposed method using data set from the Southern Great Plains of US.

2. Methodology

2.1. Instantaneous net radiation estimates

Net radiation (R_n) at the land surface can be expressed in terms of its components as

$$R_n = R_s^{\downarrow} - R_s^{\uparrow} + R_L^{\downarrow} - R_L^{\uparrow} \tag{1}$$

where $R_s^{\downarrow}$ and $R_s^{\uparrow}$ are shortwave radiation fluxes downward (W m^{-2}) and upward (W m^{-2}), respectively and $R_L^{\downarrow}$ and $R_L^{\uparrow}$ are the longwave radiation fluxes downward (W m^{-2}) and upward (W m^{-2}), respectively.

The shortwave radiation can be expressed as

$$R_s^{\downarrow} - R_s^{\uparrow} = (1-\alpha)R_s^{\downarrow} \tag{2}$$

where α is land surface reflectance (albedo).

Various parameterizations for downward shortwave radiation have been presented in the literature (Niemelä et al., 2001b). In essence, downward shortwave radiation can be expressed as

$$R_s^{\downarrow} = S_0 \tau_{sw} \cos\theta \tag{3}$$

where τ_{sw} is the atmospheric clear sky shortwave transmission factor, S_0 is the solar constant at the atmospheric top, which is about 1367 W m^{-2} and θ is the solar zenith angle.

For this study, we used the parameterization scheme developed by Zillman (1972), which uses screen level vapor pressure e_0 (hPa), and is shown in Eq. (4). Niemelä et al. (2001b) showed that Iqbal's (1983) parameterization scheme performed better than Zillman (1972), but it required information regarding transmittance by Rayleigh scattering, mixed gases, water vapor, aerosols and ozone. Such information is not readily available, thus we have used Zillman's (1972) scheme in the present study.

$$R_s^{\downarrow} = \frac{S_0 \cos^2\theta}{d} \tag{4}$$

where $d = 1.085\cos\theta + e_0(2.7+\cos\theta) \times 10^{-3} + 0.1$.

The longwave radiation can be expressed using the Steffan–Boltzmann equation as

$$R_L^{\downarrow} - R_L^{\uparrow} = \sigma\varepsilon_a T_a^4 - \sigma\varepsilon_s T_s^4 \tag{5}$$

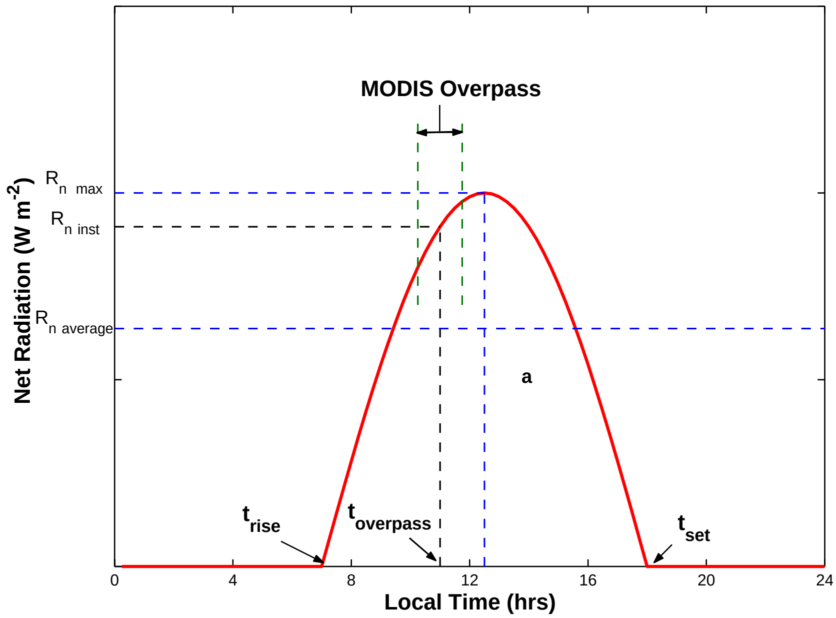

Fig. 1. The proposed sinusoidal model with MODIS overpass.

where ε_a is air emissivity, ε_s is surface emissivity, T_a is air temperature (Kelvin) at screen level, T_s is land surface temperature (Kelvin) and $\sigma=5.67\times10^{-8}$ W m^{-2} K^{-4} is the Steffan–Boltzmann constant.

Prata (1996) developed a parameterization scheme for downward longwave radiation using vapor pressure and air temperature at screen level given by Eq. (6), which provided more accurate results as compared to other schemes. Niemelä et al. (2001a), presented a review of parameterization schemes for downward longwave radiation and showed that Rapid Radiative Transfer Model (RRTM) outdid Prata's (1996) scheme in some cases. In turn RRTM divides the longwave spectrum into 16 intervals and needs information about gases like H_2O, CO_2, O_3 and others. In order to keep our methodology simple, we used Prata's (1996) scheme.

$$R_L^{\downarrow} = \varepsilon_a \sigma T_a^4 \tag{6}$$

where $\varepsilon_a=[1-(1+\xi)\exp\{-(1.2+3\xi)^{1/2}\}]$, and $\xi=46.5e_0/T_a$.

Other parameters were obtained using Terra–MODIS land data products (land surface temperature, band emissivity for bands 31 and 32, and white- and black-sky albedo) and Terra–MODIS atmospheric data products (air temperature and dew temperature at 20 different atmospheric pressure levels and aerosol depth, which is used in the computation of surface albedo). The brief description of each data products and how they were used is provided in the next section.

2.2. Diurnal cycle and daily average of net radiation estimates

Daily R_n maps certainly have more applications than INR maps, especially for models trying to estimate evapotranspiration (Jiang & Islam, 2001; Nishida et al., 2003; Norman et al., 2003). Lagouarde and Brunet (1983) proposed a framework to obtain the diurnal cycle of surface temperature by modeling it as a sinusoidal function, having a time period of day length and an amplitude equal to the difference between maximum land surface temperature and minimum air temperature. Using a similar approach as Lagouarde and Brunet's (1983) methodology, we propose a sinusoidal model for estimating the diurnal cycle of R_n for clear sky days as:

$$R_n(t) = R_{n\_max}\sin\left[\left(\frac{t-t_{rise}}{t_{set}-t_{rise}}\right)\pi\right] \tag{7}$$

where R_{n_max} is the maximum value of R_n observed during the day, t_{rise} and t_{set} is the local time at which R_n value becomes positive and negative, respectively. It should be pointed out here that t_{rise} and t_{set} are related to the local sunrise and sunset time and procedure to compute them is explained later in the text.

The proposed sinusoidal model along with MODIS overpass is shown in Fig. 1. For a given study day, INR and satellite overpass time ($t_{overpass}$) are known from model output and satellite information, thus the corresponding R_{n_max} and DANR can be given as:

$$R_{n\_max} = \frac{\text{INR}}{\sin\left[\left(\frac{t_{overpass}-t_{rise}}{t_{set}-t_{rise}}\right)\pi\right]} \tag{8}$$

and,

$$\text{DANR} = \frac{\int_{t\_rise}^{t\_set} R_n(t)\,\mathrm{d}t}{\int_{t\_rise}^{t_set} \mathrm{d}t} = \frac{2R_{n\_max}}{\pi} = \frac{2INR}{\pi sin\left[\left(\frac{t_{overpass}-t_{rise}}{t_{set}-t_{rise}}\right)\pi\right]},$$

Table 1
Ratio of daily average to instantaneous net radiation, for clear sky days, depending on the day length (T) and time difference between the Terra–MODIS overpass time and maximum net radiation (a)

T (h)	a (h)			
	0.5	1	1.5	2
8	0.65	0.69	0.77	0.9
9	0.65	0.68	0.74	0.83
10	0.64	0.67	0.72	0.79
11	0.64	0.66	0.7	0.76
12	0.64	0.66	0.69	0.74
13	0.64	0.66	0.69	0.72

thus

$$\frac{\text{DANR}}{\text{INR}} = \frac{2}{\pi \sin\left[\left(\frac{T-2a}{2T}\right)\pi\right]} \tag{9}$$

where T is day length (i.e. the difference between t_{set} and t_{rise}) and a is the difference in time between when net radiation is the maximum and when MODIS overpasses.

It can be seen from Eq. (9) that the ratio of DANR and INR is dependent on two factors, namely T and a. The day length for net radiation varied from 13 h in summer to 8 h during the winter. It was noted that the $R_{\text{n\_max}}$ generally occurred at 12:30 local time, when the ground observation data was aggregated over 15-min interval and MODIS overpass for Southern Great Plains ranged from 10:00 local time to 12:00 local time for the study period, thereby the value of a varied from 0.5 to 2.0 h. Table 1 shows the ratio of DANR and INR for combination of cases. The study days (mentioned later) cover almost the entire year, thus to avoid confusion between daylight saving time and standard time, the local time mentioned hereafter refers in standard time.

3. Terra–MODIS data products

The first EOS satellite, Terra, was launched on December 18, 1999 with MODIS as one of the five sensors onboard. Terra is at an altitude of 705 km and has a cross track and along track swath of 2330 and 10 km, respectively, with a global coverage every 1 or 2 days. It has 36 spectral bands between 0.405 and 14.385 μm whose spatial resolutions range is from 250 to 500 and 1000 m. Currently there are 44 data products and they are divided into following five sections—calibration, atmosphere, land, cryosphere and ocean. In the present study data products of calibration, atmosphere and land were used, which are available in hierarchical data format (HDF) and were obtained from EOS Data Gateway. A brief description of the data products used is given below.

3.1. Calibration data

The MODIS geolocation dataset, called MOD03, comprises of latitude, longitude, ground elevation, solar zenith angle, satellite zenith angle and azimuth angle for each MODIS 1 km pixel. The solar zenith angle is used to compute downward shortwave radiation.

3.2. Land surface temperature (LST) and emissivity data

MOD11 contains LST and band emissivities (for band 31 and 32) at spatial resolutions of 1 and 5 km, respectively for clear sky days. The generalized split-window is used to calculate LST for those pixels, whose emissivities are known in band 31 and 32 (Wan & Dozier, 1996). It is an extension of the split-window proposed by Becker and Li (1990) for AVHRR for viewing angle up to 46° from nadir, taking into account the dependence of retrieved LST on the viewing angle. The physics-based day/night LST algorithm is used to simultaneously retrieve band emissivities and temperature from a pair of daytime and nighttime MODIS observations in bands 20, 22, 23, 29, 31, 32 and 33 (Wan & Li, 1997). We have used LST data product, MOD11_L2, at 1 km spatial resolution in our study.

Wan and Dozier (1996) reported that band emissivities in AVHRR bands 4 and 5 and MODIS bands 31 and 32 are stable. Becker and Li (1990) used the average of band 4 (10.32–11.32 μm) and band 5 (11.41–12.38 μm) emissivities from AVHRR as the land surface emissivity. Land surface emissivity in the wavelength interval of 8–12 μm for the proposed methodology was calculated as average of band emissivity of MODIS band 31 (10.78–11.28 μm) and 32 (11.70–12.27 μm), given in MOD11_L2 dataset. MODIS has another band, 29, in the broadband wavelength region (8.40–8.70 μm). (MOD11B1 is another LST product, which contains band emissivities in band 20, 22, 23, 29, 31 and 32 at a 5 × 5 km spatial resolution). Wan et al. (2002) has reported that just the average of bands 31 and 32 emissivities could lead to an overestimation of land emissivity, especially in arid and semi-arid region, for which case average of all three band emissivities should be taken. It was found that an average of band emissivities in channels 29, 31 and 32 was not significantly different from the average of band emissivity of channels 31 and 32. Our study site is primarily wet and moreover the error in INR due to changes in land surface emissivity does not appear to be large. Thus we have used average of band emissivity 31 and 32 to represent land surface emissivity.

3.3. Land surface albedo data

The MODIS bidirectional reflectance distribution function (BRDF) and albedo product, called MOD43B, is an MODIS standard data product that began routine production in 2000, shortly after the launch of Terra. These data products are produced every 16 days at a 1 km spatial resolution and archived as equal area titles representing of 1200 × 1200 pixels in sinusoidal (V004) and integrated sinusoidal (V003) projections. Currently three products are available—BRDF model parameters (MOD43B1), global

Table 2
Coefficients to convert MODIS narrowband albedo to shortwave albedo (Liang et al., 1999)

MODIS bands	Coefficients
1	0.3973
2	0.2382
3	0.3489
4	−0.2655
5	0.1604
6	−0.0138
7	0.0682
Intercept	0.0036

albedo (MOD43B3) and nadir–BRDF adjusted reflectance (MOD43B4) (Schaaf et al., 2003).

In the present study, we have used MOD43B3 V004 data product, which consist of black- and white-sky albedos for seven spectral bands (band 1–7) and the three broadbands (0.30–0.7, 0.7–3.0 and 0.3–5.0 μm). Black- and white-sky albedos mark the extreme cases of completely direct and diffuse illumination. Actual albedo, $\alpha(\theta,\lambda)$, for each band, can be calculated as the interpolation between these two values depending on the aerosol depth (τ), as

$$\alpha(\theta,\lambda) = \{1 - S(\theta,\tau(\lambda))\}\alpha_{bs}(\theta,\lambda) + S(\theta,\tau(\lambda))\alpha_{ws}(\theta,\lambda) \quad (10)$$

where $\alpha_{bs}(\theta,\Lambda)$ is black-sky albedo, $\alpha_{ws}(\theta,\Lambda)$ is white-sky albedo, $S(\theta,\tau(\Lambda))$ is the isotropic fraction, a representation of atmospheric state, θ is the solar zenith angle and Λ is the waveband of the channel (Lucht et al., 2000).

Table 3
Geographic location of ground stations in Southern Great Plains

Station no.	Latitude (N)	Longitude (W)
E1	38.202	99.316
E3	38.201	95.597
E4	37.953	98.329
E5	38.114	97.513
E6	37.842	97.020
E7	37.383	96.180
E8	37.333	99.309
E9	37.133	97.266
E10	37.068	95.788
E11	36.811	98.285
E12	36.841	96.427
E13	36.605	97.427
E15	36.431	98.284
E16	36.061	99.134
E18	35.687	95.856
E19	35.557	98.017
E20	35.564	96.988
E24	34.883	98.204

To compute the isotropic fraction, $S(\theta,\tau(\Lambda))$, a look up table (LUT) has been generated with the help of 6S code (atmospheric radiative transfer code). The LUT is precalculated for 90 solar zenith angles (0° to 89° with a step of 1°), 50 optical depths (0–1.0 with a step of 0.02), 10 bands (7 MODIS spectral bands and 3 broadbands) and 2 aerosol models (continental and maritime). The LUT is available from MODIS BRDF/albedo products homepage (http://geography.bu.edu/brdf/). The optical depth used for the generation of LUT is based on the wavelength at 0.550 μm

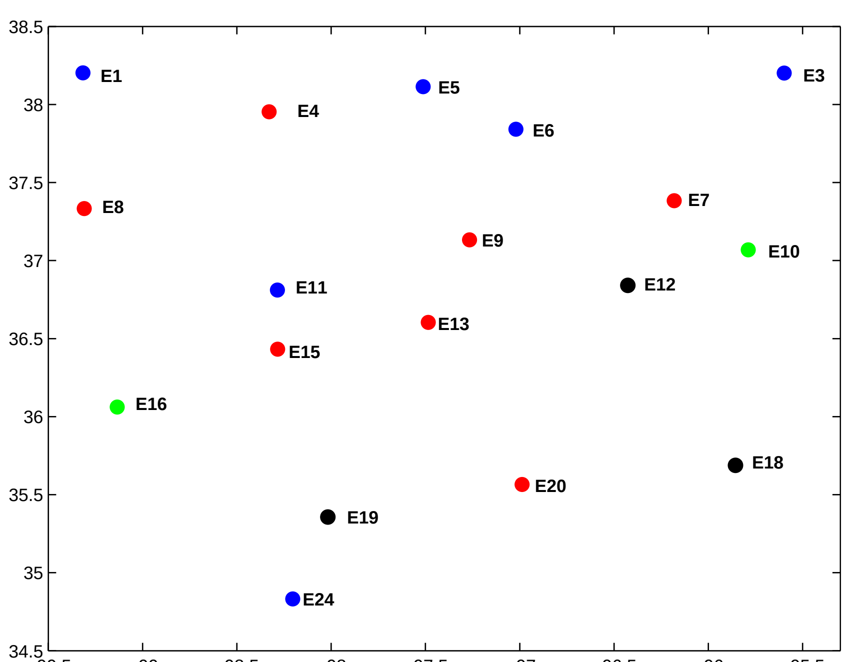

Fig. 2. Distribution of ground stations in the Southern Great Plains. Various colors represents ground stations measuring various quantities (a) black stations—recorded net radiation and shortwave radiation; (b) blue stations—recorded air temperature and shortwave radiation; (c) green stations—recorded only shortwave radiation; and (d) red stations—recorded net radiation, shortwave radiation and air temperature.

Table 4
Terra overpass time for the study days

Calendar day (Julian day)	Over pass time, UTC	Sunrise time (standard time)	Sunset time (standard time)
19th January (019)	17:45 and 17:50	7:39	17:41
23rd March (082)	17:05	6:29	18:43
24th March (083)	17:45 and 17:50	6:27	18:44
31st March (090)	17:55	6:17	18:15
1st April (091)	17:00	6:15	18:51
9th April (099)	17:45 and 17:50	6:04	18:58
10th April (100)	16:50 and 16:55	6:02	18:59
20th April (110)	17:30	5:51	19:08
6th September (249)	17:10	6:04	18:57
19th September (262)	16:40	6:14	18:31
20th September (263)	17:20	6:15	18:30
12th October (285)	16:45	6:33	17:57
15th October (288)	17:15	6:36	17:53
19th October (292)	16:50	6:40	17:48
22nd October (295)	17:20 and 17:25	6:41	17:46

and this is also available as MODIS aerosol depth product, discussed later in this section.

To compute shortwave albedo from narrowband albedos, a linear combination of 7 MODIS spectral band was carried out. The coefficients, shown in Table 2, were obtained from Liang et al. (1999), which have been shown to estimate shortwave albedo accurately.

3.4. Air and dew point temperature data

The MODIS atmospheric profile product (MOD07) provides several parameters, of which air and dew point temperature profiles were used in the current study. The spatial resolution of this product is 5×5 km, at 20 vertical atmospheric pressure levels and it is produced daily. MOD07 uses a statistical regression retrieval algorithm to determine the temperature profiles, using previously determined statistical relationship between the observed radiances and the corresponding atmospheric profiles. The statistical retrieval algorithm uses 12 MODIS spectral bands (24–25 and 27–36). The method, as done in the International TOVS Processing Package, is used to produce first guess for a physical retrieval process (Menzel et al., 2002).

In the present study, air temperature and dew point temperature at vertical pressure level of 1000 hPa, are taken as surrogate for the temperatures at screen level height. Also the temperatures are assumed to homogenous over the 5×5 km grid. Dew point temperature is used to compute the vapor pressure, e_0 (hPa), by using the Clausius–Clapeyron equation as:

$$e_0 = 6.11\exp\left[\frac{L_v}{R_v}\left(\frac{1}{T_0}-\frac{1}{T_d}\right)\right] \tag{11}$$

where L_v is the latent heat of vaporization (2.5×10^6 J kg^{-1}), R_v is the gas constant for water vapor (461 J kg^{-1} K^{-1}) and T_0=273 K.

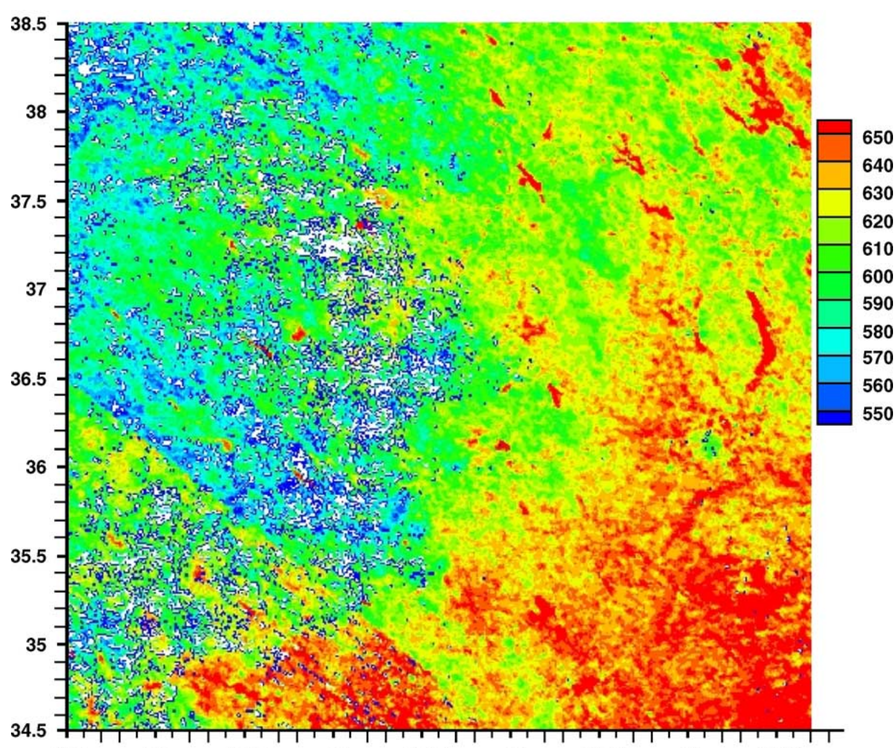

Fig. 3. A typical instantaneous net radiation map (in W m^{-2}) for 6th September 2003. Region in white represents where no information was available due to cloud cover.

3.5. Aerosol depth data

MODIS aerosol product (MOD04) monitors ambient aerosol thickness over oceans and over portion of continents. This data product is provided daily at a spatial resolution of 10 × 10 km pixel array. The aerosol depth over land is estimated using dark target approach. The algorithm takes advantage of MODIS wide spectral and high spatial resolution bands with global coverage (e.g. bands 1 and 2 at 250 m, bands 3–7 at 500 m and band 20 at 1 km). It also requires prior cloud screening using MODIS data. The dynamic aerosol models will be derived from ground-based sky measurements and is used in the net retrieval process (Kaufman & Tanré, 1998). In the current study the aerosol depth was assumed to be homogeneous over the 10 × 10 km grid. The aerosol depth is estimated for three wavelengths—0.470, 0.550 and 0.659 μm. The one at 0.550 μm was used for the computation of land surface albedo, as mentioned earlier.

At this time, it should be mentioned that all the data products were MODIS level 2 (swath) data except land surface albedo, which was a 16-day composite global MODIS level 3 (gridded) data. The land surface albedo is assumed constant during this 16-day interval. We must note, however, that if vegetation cover changes significantly during the 16-day interval, then it could cause errors in land surface albedo estimates. The MODIS level 3 data (albedo data) is archived in predefined tiles, each consisting of 1200 × 1200 pixels. MODIS Land Science team (MODLAND) have developed software called MODLAND Tile Mapper, which calculates the latitude and longitude of any pixel in any given tile in various map projections (e.g. sinusoidal, integrated sinusoidal and Goodes Homolosine). The latitude and longitude for the pixels in MOD43B3 dataset were obtained by executing the precompiled output file of MODLAND Tile Calculator, for a pixel size of 1 km. The land surface albedo, for each day, was then re-projected using the nearest neighbor scheme onto the other datasets.

Table 5
Bias, root mean square error (RMSE) and correlation (R^2) for air temperature, shortwave downward flux and net radiation

	Bias (=modeled – observed)	RMSE	R^2
T_a (°C)	−2.07	5.01	0.62
$R_s^{\downarrow}$(W/m^2)	41	51	0.97
Instantaneous R_n(W m^{-2})	59	74	0.89
Daily average R_n(W m^{-2})	50	60	0.85

4. Application of the algorithm over Southern Great Plains

4.1. Study site and data description

The study site is over the Southern Great Plains (SGP), covering most of the Oklahoma and southern part of Kansas. It extends in latitude from about 34.5° to 38.5 °N and in longitude from 95.3° to 99.5° W. Fig. 2 shows the various ground stations, which were used to validate the study. The Atmospheric Radiation Measurement (ARM) Program maintains the ground stations and Table 3 summarizes their geographic locations. The dimensions of the defined area in Fig. 2 are 444 rows by 467 columns with pixel resolution 1 km, having a grid interval of 0.009° in

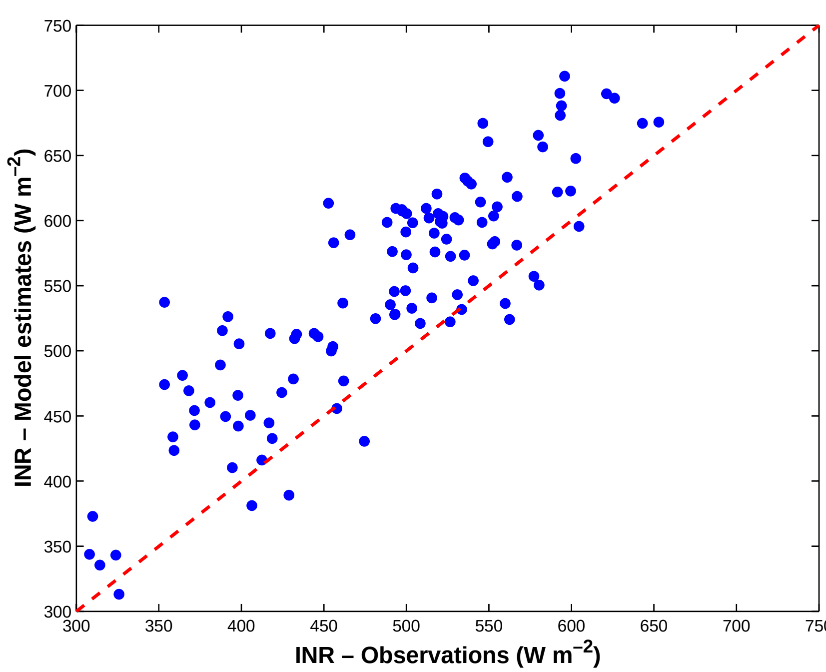

Fig. 4. Comparison of observed and modeled instantaneous net radiation estimates for all study days.

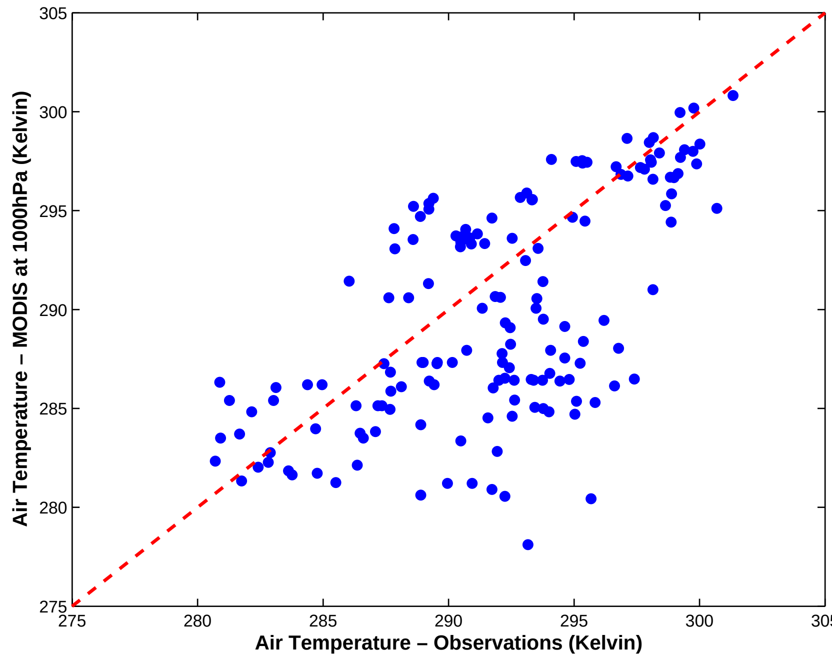

Fig. 5. Comparison of observed and retrieved air temperature from MODIS data product (MOD07) at 1000 hPa level for all study days.

both latitude and longitude. Shortwave radiation and air temperature measurements were recorded at 1-min time interval, while net radiation was available at 5-min time intervals. All the observations were averaged over 15-min time interval for the purpose of validation. In Fig. 2, the stations shown in 'black' recorded net radiation and shortwave radiation measurements; those in 'blue' recorded air temperature and shortwave radiation; those in 'green' recorded only shortwave radiation; and those in 'red' measured all the three quantities.

The MODIS datasets used for the study consists of MODIS level-2 data (during the day overpass)—MOD03, MOD04, MOD07 and MOD11_L2; and MODIS level-3 data—MOD43B3. The methodology was applied to fifteen clear sky days for MODIS overpass in the year 2003, which range from late winter to late fall. The criteria for determining a clear sky was that 80% of the study region should be free from cloud cover. The MOD11_L2 data product is available for only clear sky pixels, thus counting the number of pixels in MOD11_L2

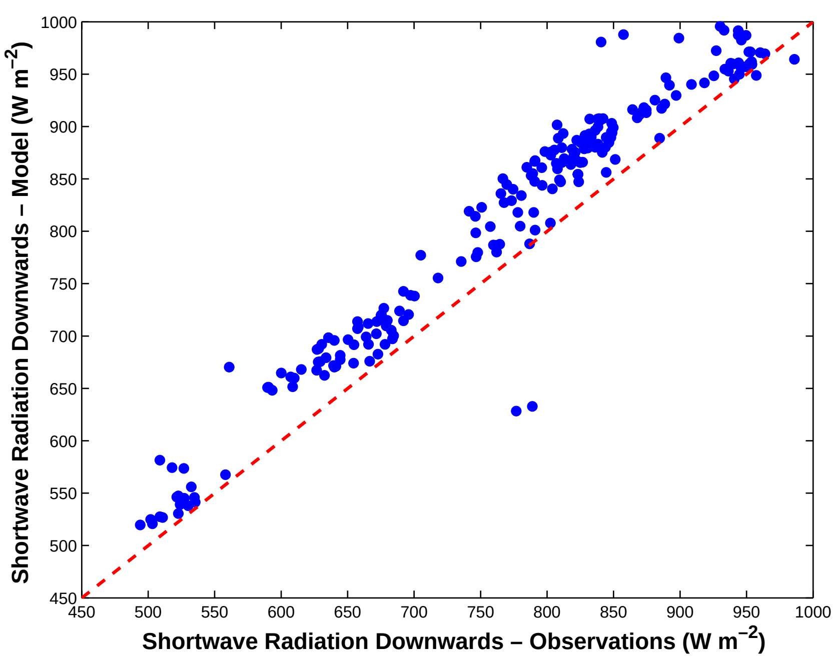

Fig. 6. Comparison of observed and estimated shortwave radiation downwards using Zillman's scheme for all study period.

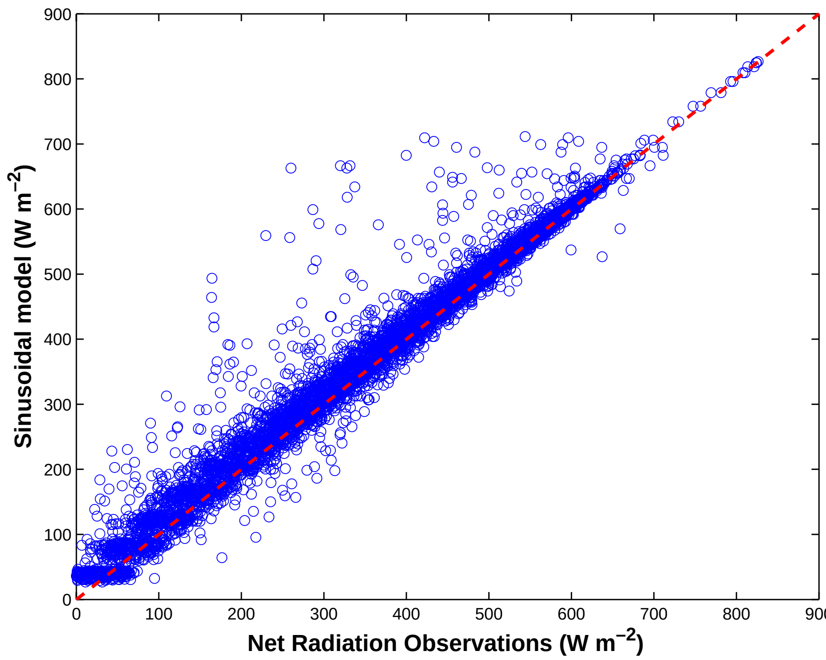

Fig. 7. Comparison of diurnal cycle net radiation observations and sinusoidal model at 15-min time step for the entire study period.

for which land surface temperature was available served as an indicator of the cloud cover over the study site. Table 4 gives the description of study period and satellite overpass time over the study region for each day. Each MODIS scene (level 1 and 2 data) is constructed from 203 or 204 scans along track, sampled at 1354 times in the cross track direction, corresponding to 5 min of data. Each individual MODIS scan contains 10 along track spatial elements. Thus for few study days, the SGP got split in two MODIS scene, which were separated by 5 min. It should be noted that splitting of the study region into two MODIS scene has no effect on the land surface albedo data (level 3) as albedo data are obtained from predefined tiles.

The third and fourth column of Table 4, contains the sunrise and sunset time (standard time) for the study region, obtained from the website of US Naval Observatory, Astronomical Application Department (http://aa.usno.navy.mil/), which are used in the estimation of the diurnal cycle of net radiation.

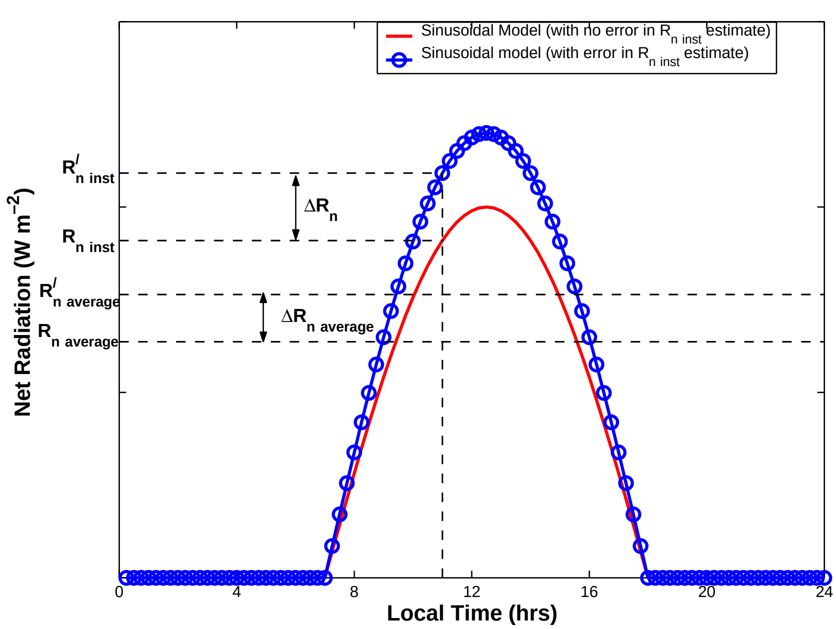

Fig. 8. Error in the estimation of daily average net radiation.

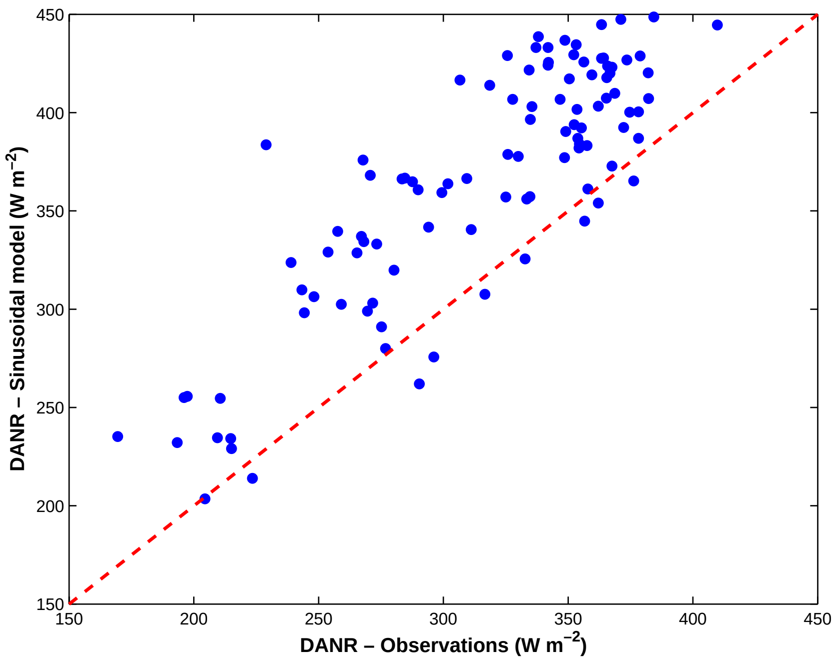

Fig. 9. Comparison of observed and modeled daily average net radiation estimates using sinusoidal model for entire study period.

4.2. Results and validation

4.2.1. Instantaneous net radiation estimates

The INR radiation maps are obtained using the scheme discussed is Section 3. An example of the INR map for the study domain on 6th September, 2001, is shown as Fig. 3. The white region in the map refers to the area that had cloud cover. We must emphasize that our goal is to obtain net radiation maps over large areas, and we note that there are no generally accepted methodologies to compare spatially distributed maps with point-based ground observation. Ground observation data are generally discrete and limited in number and also the measurement error associated with such measurements should be kept in mind, while doing such comparisons.

The comparison between the observed and the modeled INR is shown in Fig. 4. The bias, root mean square error (RMSE) and correlation (R^2) for air temperature, shortwave downward and instantaneous net radiation for all available stations is shown in Table 5. The error in the net radiation and shortwave radiation down is approximately of the order of 14% and 6% of the ground observations. Jacobs et al. (2000) have performed a similar study of estimating net radiation from GOES and compared their results with pyranometer estimates. They reported bias, RMSE and R^2 for INR as 73.5 W m^{-2}, 107.7 W m^{-2} and 0.75, while our results have a bias, RMSE and R^2 of 59 W m^{-2}, 74 W m^{-2} and 0.89. respectively (as shown in Table 5). It should be noted that Jacobs et al. (2000) performed the study for one ground station while assuming a fixed value of surface emissivity and land surface albedo. The methodology developed in this paper is capable of estimating INR over a heterogeneous domain. On the other hand, Jacobs et al. (2000) have applied their methodology for cloudy sky conditions too; while the framework presented here is only applicable for clear sky cases. Other researchers reported similar magnitude of uncertainty. As examples, Ma et al. (2002) stated a mean absolute percent difference in R_n estimate as 7.5%, while using the radiative transfer model, MODTRAN, and Norman et al. (2003) reported an error of 50 W m^{-2} for R_n.

The comparison of air temperature observed and that obtained from MODIS data product (MOD07) at 1000 hPa for all ground stations during the study period is shown in Fig. 5, with a bias, RMSE and R^2 of -2.07 °C, 5.01 °C and 0.62. The modeled air temperature is underestimated which could be due to the fact that the air temperature in MOD07 at 1000 hPa level does not truly represent the air temperature at screen level height. Fig. 6 shows the comparison of ground observations and estimated shortwave radiation downwards using Zillman's (1972) scheme, which had a bias, RMSE and R^2 of 41 W m^{-2}, 51 W m^{-2} and 0.97. A systematic bias in shortwave estimate is evident from Fig. 6. Niemelä et al. (2001b) have also shown that for values of solar zenith angle less than 40°, Zillman's (1972) scheme overestimates the downward shortwave radiation. The solar zenith angle for our study period was always less than 40°. After removing this systematic bias from shortwave radiation; the bias, RMSE and R^2 for instantaneous net radiation are 24 W m^{-2}, 50 W m^{-2}, and 0.89. Overall, the proposed methodology provides R_n over heterogeneous area with comparable accuracy as those of current methods. This methodology is perhaps one of the first attempts to develop an algorithm which solely uses remote sensing information and eliminates the need for ancillary ground information as model input.

4.2.2. Diurnal cycle and daily average net radiation estimates

The proposed sinusoidal model, similar to Lagourade and Brunet's (1983) model, to estimate diurnal cycle of R_n for clear sky requires information regarding the time when the R_n starts to rise and becomes greater than zero (t_{rise}) and also the time when it again becomes less than zero (t_{set}). It has been observed that R_n generally starts to increase about 45 min after sunrise and it becomes less than zero about 45 min before sunset, for the entire range of study period. We acknowledge that for some cases such an estimation of t_{rise} and t_{set} might be inaccurate, but the errors in final estimation of DANR due to this are small enough to neglect. The variation in the sunrise and sunset time for all the ground stations in the study region was less than 15 min. Thereby one value of sunrise and sunset time was chosen for whole domain as given in Table 4.

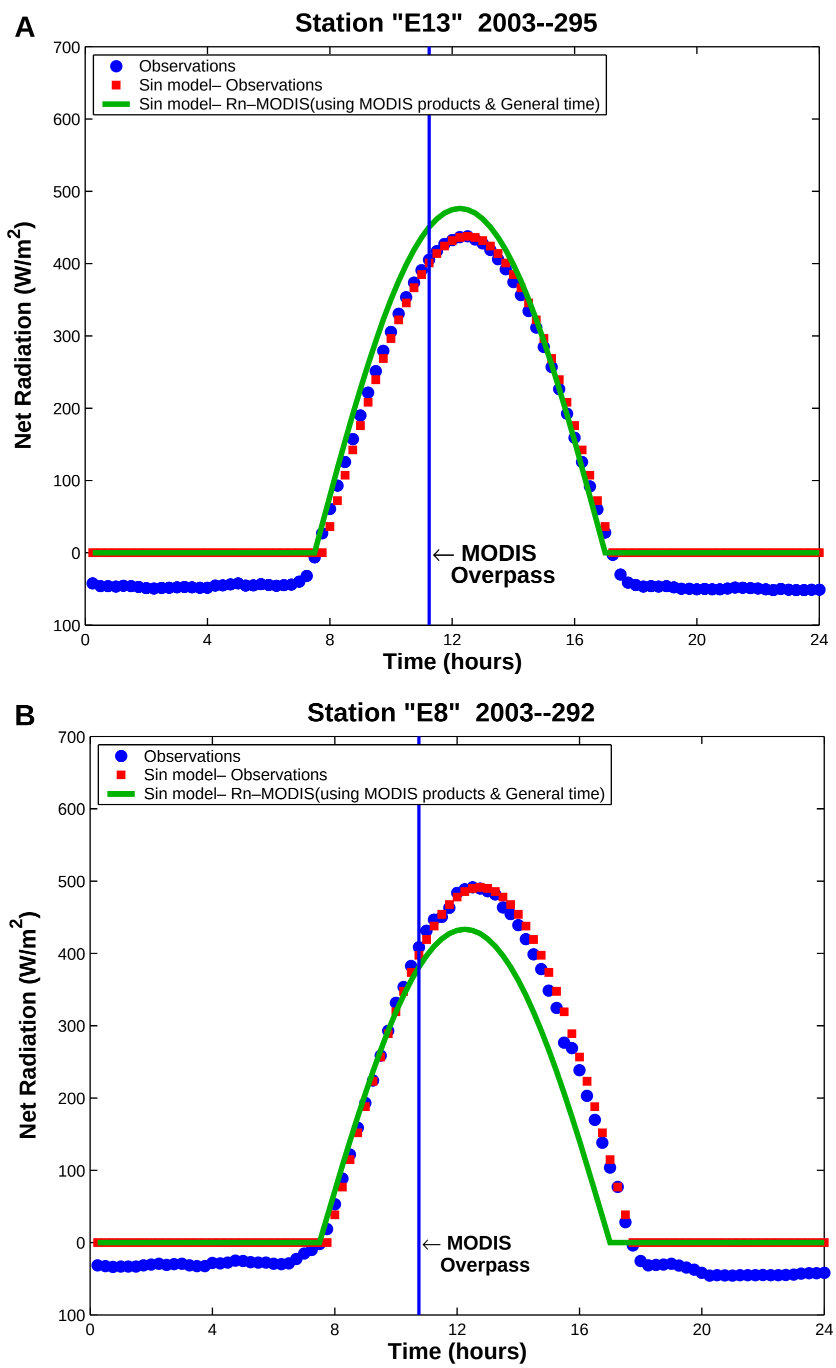

Fig. 10. (A) Diurnal cycle of net radiation when instantaneous R_n had an error. (B) Diurnal cycle of net radiation, showing the impact of the time period of sinusoidal model. (C) Diurnal cycle of net radiation retrieved accurately.

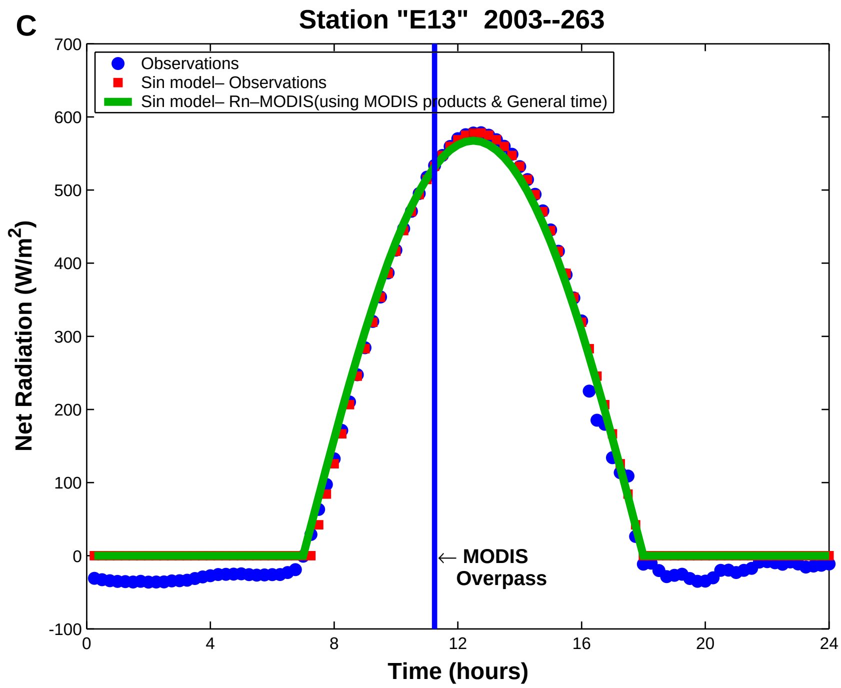

Fig. 10 (*continued*).

4.2.2.1. Applicability of sinusoidal model. The sinusoidal model is first applied to the ground observations of all stations recording R_n values for the entire study period to examine the accuracy of the proposed method. In each case, $R_{n\text{–}max}$ was taken as the maximum observation recorded by that particular station on a given day. The sunrise and sunset time, given in Table 4, were used to compute t_{rise} and t_{set} as mentioned earlier. R_n values were estimated at 15-min time step and compared to ground observations which was also aggregated to 15 min, as shown in Fig. 7. The bias, RMSE and R^2 were 21 W m^{-2}, 45 W m^{-2} and 0.98, suggesting that sinusoidal model is acceptable to retrieve diurnal cycle of net radiation. It should be also pointed out that some study periods were clear sky days for the Terra–MODIS overpass but had clouds either before or after Terra–MODIS overpass. Fig. 7 is generated disregarding whether clouds were present over the stations at anytime during the day. If only those study days are considered, which did not have any cloud cover during the whole day, then the bias, RMSE and R^2 for sinusoidal model and observations were 14 W m^{-2}, 28 W m^{-2} and 0.99.

4.2.2.2. Daily average net radiation estimates. The DANR estimates should have a lower RMSE compared to INR estimates, as explained in Fig. 8. Let the error in the estimation of INR (ΔR_n) be +15%, which implies that the retrieved diurnal cycle (with circles in blue) is 1.15 times the actual diurnal cycle (in red). It can be inferred from Table 1, the ratio of DANR to INR for varying values of daytime length and Terra–MODIS overpass time, that for all cases MODIS overpasses the study region at the time after the DANR value is achieved (as shown in Fig. 1). Thus, the error in the estimation of DANR ($\Delta R_{n\ average}$) would also be +15%, but having a lower magnitude of error. The comparison between the observed and modeled DANR estimates for the entire study period is shown in Fig. 9. The RMSE, bias and R^2 for the DANR values are 50 W m^{-2}, 60 W m^{-2} and 0.85 (as shown in Table 5); which indicates that the daily average estimates of net radiation as compared to instantaneous will have a lower magnitude of error.

4.2.2.3. Diurnal cycle of net radiation estimates. The diurnal cycle of net radiation estimated using the proposed sinusoidal is shown in Fig. 10. In all the cases, the sinusoidal model using observations (shown in red box) matched extremely well with the observations (shown in blue circles). The error in INR affects the diurnal cycle retrieval is shown in the first case, while second case highlights that in some cases the estimation of t_{rise} and t_{set} (general time) as 45 min after and before sunrise might not be accurate. Third case shows when diurnal cycle was retrieved accurately using the sinusoidal model. Overall the proposed sinusoidal model is able to capture the diurnal variation in net radiation for clear sky days.

5. Summary and discussion

In this study, we have developed a stand-alone methodology to estimate instantaneous and daily average net radiation over large heterogeneous areas for clear sky days. The methodology attempts to overcome two major shortcomings of the current INR models by using only remote sensing information. It eliminates the need for ground data as model input, and also explicitly recognizing the need of spatially varied input parameters. The methodology exploits the various land data products (land surface temperature, land surface emissivity and land surface albedo) and atmospheric data products (air temperature, dew temperature and aerosol depth) from Terra–MODIS. Zillman's (1972) and Prata's (1996) parameterization schemes were used to estimate downward shortwave flux and air emissivity.

Due to limited applicability of instantaneous net radiation estimates compared to daily average value or diurnal cycle of R_n, a sinusoidal model is proposed to estimate the diurnal variations of R_n. The sinusoidal model is capable of retrieving the diurnal variation of R_n with a single INR estimate from satellite. The proposed methodology was tested over Southern Great Plains for fifteen clear sky days in 2003. The results from this study are comparable to or better than currently available R_n estimation methodologies that use ground-based observa-

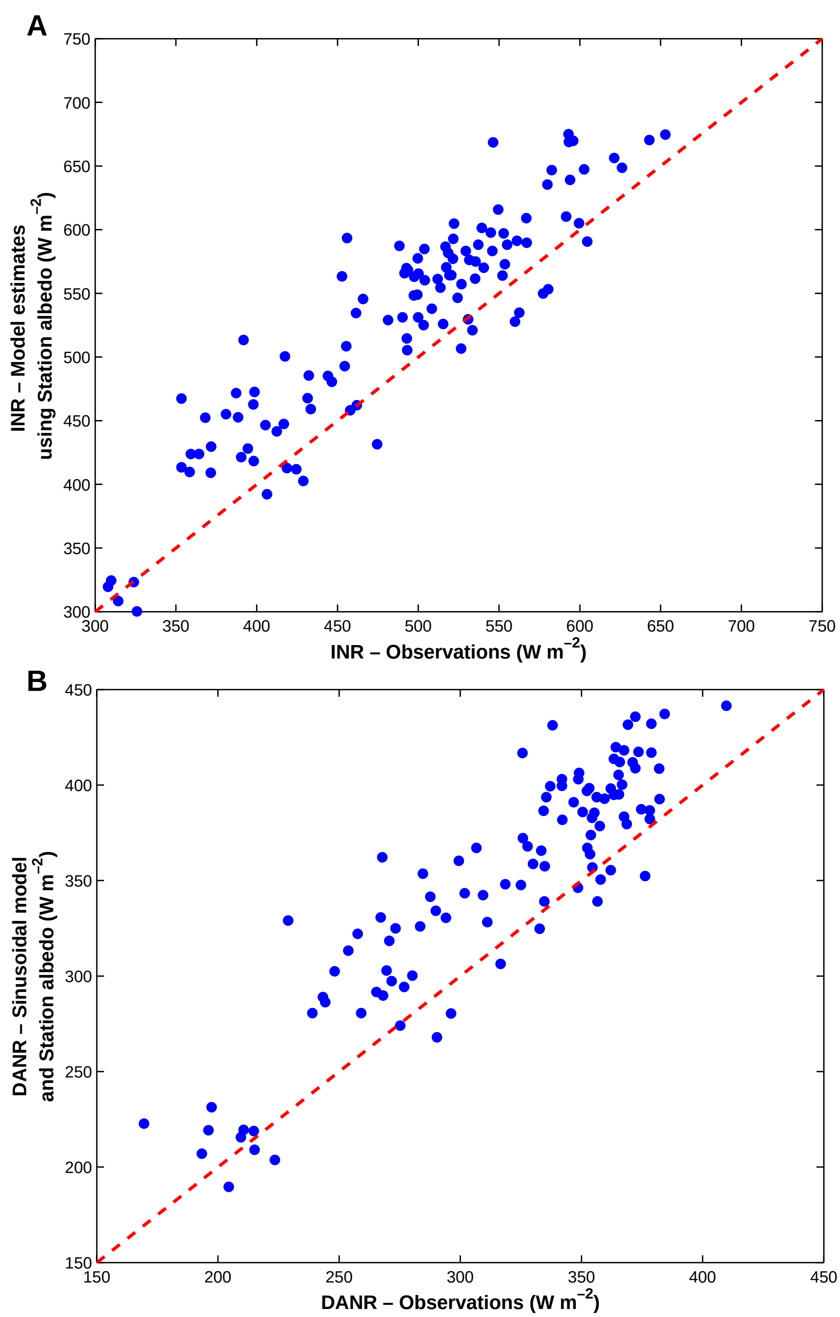

Fig. 11. (A) Comparison of observed and estimated instantaneous net radiation using ground station albedo values for entire study period. (B) Comparison of observed and estimated daily average net radiation using ground station albedo values of entire study period.

tions (Jacobs et al., 2000; Ma et al., 2002; Norman et al., 2003).

We enumerate several sources of error that may affect operational estimation and implementation of proposed net radiation algorithm from MODIS sensors:

1) Wan et al. (2002) have validated MODIS-LST MOD11_L2 product over lakes and vegetation areas. The errors for surface temperature estimation compared to in situ observations over lakes are reported to be less than 1 K. While for uniform vegetated sites, with little variation in soil moisture and surface temperature spatially, the MODIS-LST are few Kelvin degrees lower than in situ measurements, which could be attributed to overestimation of land surface emissivity in semi-arid and arid areas from land cover types in the split-window LST method. Thus it is possible to encounter an error larger than 1 K in MODIS-LST over heterogeneous area.
2) While applying the proposed methodology to semi-arid and arid areas, care should be taken in estimating land surface emissivity. Wan et al. (2002) have reported that an average of bands 31 and 32 emissivities could lead to an overestimation of land emissivity, especially in arid and semi-arid region. MODIS has another band, 29, in the broadband wavelength region (8.40–8.70 μm) and an average of all three band emissivities should be taken. (MOD11B1 is another LST product, which contains band emissivities in bands 20, 22, 23, 29, 31 and 32 at a 5 km spatial resolution).
3) The air and dew point temperature from MOD07 temperature profile product at 1000 kPa are taken as surrogate for temperatures at the screen level height. These temperatures at 1000 kPa level might not truly correspond to a screen level height. If information regarding the height of 1000 kPa level above the ground surface is available, then the temperature profile could be extrapolated to compute air temperature at screen level height.
4) The methodology uses a 16-day surface albedo product, MOD43B3, if the vegetation cover changes during this 16-day period interval then land surface albedo estimates are likely to introduce error in net radiation estimates.
5) Comparison of shortwave radiation estimates using Zillman's (1972) scheme and ground measurements suggests a systematic bias. This is consistent with the results presented in Niemelä et al. (2001b), which shows that for low values of solar zenith angle, Zillman's schemes overestimates shortwave radiation.
6) Finally, the model results were compared with ground observations, while assuming that the ground flux stations represent the same sample spatial scale as that of the remotely derived values. This assumption could lead to large discrepancies when ground stations are located in a heterogeneous area. The issues related to scale of measurement and comparison metrics needs further exploration for the validation of remote sensing algorithm using ground-based observations.

The error in 16-day land surface albedo product was most significant in determining the accuracy of R_n. Fig. 11 shows comparison of ground observations with INR and DANR estimates, which were calculated using land surface albedo from ground stations, while all other parameters

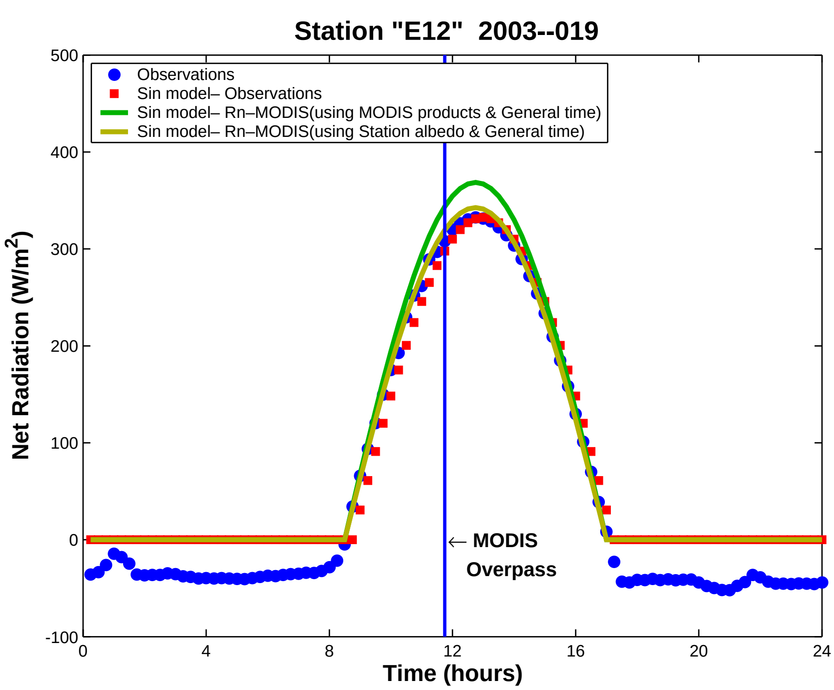

Fig. 12. Diurnal cycle of net radiation using station albedo.

from MODIS data products. Ground station albedo was estimated as the ratio of hemispherical shortwave radiation downwards to hemispherical shortwave upwards around noon. When using ground station albedo, the RMSE, bias and R^2 for INR were 40 W m^{-2}, 53 W m^{-2} and 0.93; while for DANR estimates they are 36 W m^{-2}, 45 W m^{-2} and 0.91. In both cases bias and RMSE have decreased, while R^2 had a slight increase compared to cases when MODIS 16-day albedo product is used, suggesting more accurate information regarding land surface albedo can improve the proposed methodology. Fig. 12 shows that the retrieved diurnal cycle of net radiation, using ground station albedo observations, was able to capture the variations of net radiation more accurately than using MODIS 16-day land surface product.

We acknowledge that the current method uses simple parameterization schemes to compute shortwave radiation downwards and air emissivity and does not involve a complex radiative transfer model. Nonetheless, the proposed methodology appears to retrieve R_n for clear sky days with comparable accuracy to those of current methods that use ground-based observations and mainly provides point estimates. In a cloudy day scenario, the diurnal cycle of R_n cannot be retrieved from one instantaneous R_n estimate from polar orbiting satellite but simultaneous use of R_n estimates from other sensors (like Geostationary Operational Environmental Satellite, Advanced Very High Resolution Satellite) will be needed to retrieve the diurnal cycle of R_n.

In summary, a simple scheme is proposed to estimate net radiation, both instantaneous and daily average values for clear sky days. It tries to overcome the need for ground information as model input by exploiting Terra–MODIS land and atmospheric data product. It explicitly recognizes the need for spatially varied parameters. The future research work would aim at utilizing the retrieved net radiation estimates using the proposed methodology as a component to obtain evapotranspiration estimates.

Acknowledgment

This work was supported, in part, by grants from the National Research Institute Competitive Grants Program (MASR-2004-00888) and the National Aeronautics and Space Administration (NAG5-11684).

References

Bastiaanssen, W. G. M., Pelgrum, H., Menenti, M., & Feddes, R. A. (1996). Estimation of surface resistance and Priestley–Taylor α-parameter at different scales. In J. Stewart, E. Engman, R. Feddes, & Y. Kerr (Eds.), *Scaling up in hydrology using remote sensing* (pp. 93–111). New York: Wiley.

Becker, F., & Li, Z. L. (1990). Towards a local split window method over land surfaces. *International Journal of Remote Sensing*, *11*(3), 369–393.

Diak, G. R., & Gautier, C. (1983). Improvements to a simple physical model for estimating insolation from GOES data. *Journal of Climate and Applied Meteorology*, *22*, 505–508.

Ellingson, R. G. (1995). Surface longwave fluxes from satellite observations: A critical review. *Remote Sensing of Environment*, *51*, 89–97.

Gautier, C., Diak, G., & Masse, S. (1980). A simple physical model to estimate incident solar radiation at the surface from GOES satellite data. *Journal of Applied Meteorology*, *19*, 1005–1012.

Hurtado, E., & Sobrino, J. A. (2001). Daily net radiation estimated from air temperature and NOAA–AVHRR data: A case study for the Iberian Peninsula. *International Journal of Remote Sensing*, *22*(8), 1521–1533.

Islam, S., Eltahir, E., & Jiang, L. (2003). *Final report on satellite based evapotranspiration estimation for South Florida Water Management District* (pp. 74).

Iqbal, M. (1983). *An introduction to solar radiation* (pp. 169–213). Academic Press.

Jackson, R. D., Reginato, R. J., & Idso, S. B. (1977). Wheat canopy temperature: A practical tool for evaluating water requirements. *Water Resources Research*, *13*, 651–656.

Jacobs, J. M., Myers, D. A., Anderson, M. C., & Diak, G. R. (2000). GOES surface insolation to estimate wetlands evapotranspiration. *Journal of Hydrology*, *266*, 53–65.

Jiang, L., & Islam, S. (2001). Estimation of surface evaporation map over southern Great Plains using remote sensing data. *Water Resources Research*, *37*(2), 329–340.

Kaufman, Y., & Tanré, D., 1998 Algorithm for remote sensing of tropospheric aerosol from MODIS. ATBD Reference Number: ATBD-MOD-02. http://modis.gsfc.nasa.gov/data/atbd/atbd_mod02.pdf (accessed on 12/04/2003).

Lagouarde, J. P., & Brunet, Y. (1983). A simple model for estimating the daily upward longwave surface radiation flux from NOAA–AVHRR data. *International Journal of Remote Sensing*, *14*(5), 907–925.

Liang, S., Strahler, A. H., & Walthall, C. (1999). Retrieval of land surface albedo from satellite observations: A simulation study. *Journal of Applied Meteorology*, *38*(6), 712–725.

Lucht, W., Schaaf, C. B., & Strahler, A. H. (2000). An algorithm for the retrieval of albedo from space using semiempirical BRDF models. *IEEE Transactions on Geoscience and Remote Sensing*, *38*(2), 977–998.

Ma, Y., Su, Z., Li, Z., Koike, T., & Menenti, M. (2002). Determination of regional net radiation and soil heat flux over a heterogeneous landscape of the Tibetan Plateau. *Hydrological Processes*, *16*, 2963–2971.

Menzel, W. P., Seemann, S. W., Li, J., Gumley, L. E., (2002). MODIS atmospheric profile retrieval algorithm theoretical basis document, Version 6, Reference Number: ATBD-MOD-07. http://modis.gsfc.nasa.gov/data/atbd/atbd_mod07.pdf (accessed on 12/04/2003).

Niemelä, S., Räisänen, P., & Savijärvi, H. (2001a). Comparison of surface radiative flux parameterizations: Part I. Longwave radiation. *Atmospheric Research*, *58*, 1–18.

Niemelä, S., Räisänen, P., & Savijärvi, H. (2001b). Comparison of surface radiative flux parameterizations: Part II. Shortwave radiation. *Atmospheric Research*, *58*, 141–154.

Nishida, K., Nemani, R. R., Running, S. W., & Glassy, J. M. (2003). An operational remote sensing algorithm of land evaporation. *Journal of Geophyscial Research*, *108*(D9), 4270.

Norman, J. M., Anderson, M. C., Kustas, W. P., French, A. N., Mecikalski, J., Torn, R., et al. (2003). Remote sensing of surface energy fluxes at 10^1-m pixel resolutions. *Water Resources Research*, *39*(8), 1221.

Pinker, R. T., Frouin, R., & Li, Z. (1995). A review of satellite methods to derive surface shortwave irradiance. *Remote Sensing of Environment*, *51*, 108–124.

Prata, A. J. (1996). A new long-wave formula for estimating downward clear-sky radiation at the surface. *Quarterly Journal of the Royal Meteorological Society*, *122*, 1127–1151.

Schaaf, C. B., Gao, F., Strahler, A. H., Lucht, W., Li, X., Tsang, T., et al. (2003). First operational BRDF, albedo nadir reflectance product from MODIS. *Remote Sensing of Environment*, *83*, 135–148.

Seguin, B., Assad, E., Freaud, J. P., Imbernon, J. P., Kerr, Y., & Lagouarde, J. P. (1989). Use of meteorological satellite for rainfall and evaporation monitoring. *International Journal of Remote Sensing*, *10*, 1001–1017.

Wan, Z., & Dozier, J. (1996). A generalized split-window algorithm for retrieving land-surface temperature from space. *IEEE Transactions of Geoscience and Remote Sensing*, *34*(4), 892–905.

Wan, Z., & Li, Z. L. (1997). A physics-based algorithm for retrieving land-surface emissivity and temperature from EOS/MODIS data. *IEEE Transactions of Geoscience and Remote Sensing*, *35*(4), 980–996.

Wan, Z., Zhang, Y., Zhang, Q., & Li, Z. (2002). Validation of the land-surface temperature products retrieved from Terra Moderate Resolution Imaging Spectroradiometer data. *Remote Sensing of Environment*, *83*, 163–180.

Zillman, J. W. (1972). A study of some aspects of the radiation and heat budgets of the southern hemisphere oceans. *Meteorol. Studyl 26, Bur. Of Meteorol.*. Canberra, Australia: Dept. of the Inter.